

# Appendix S1

1 James and Gray (1986) have shown a reduction in the amount of eddy kinetic energy  
2 with increasing surface friction time scales. For the present model experiments, this finding  
3 is confirmed by Figures 1, 2, and 3. Specifically, they show the standard deviation at every  
4 gridpoint, or the square root the time-mean, zonal-mean squared anomalies  $[\overline{u'^2}]^{1/2}$  and  
5  $[\overline{\omega'^2}]^{1/2}$  of zonal and vertical velocity  $u$  and  $\omega$  and time-mean, zonal-mean variance  $[\overline{v^{*2}}]$   
6 of bandpass filtered meridional velocity  $v^*$ , where brackets and the overbar denote a zonal  
7 or temporal average and the prime denotes the departure from that mean at every grid-  
8 point. To promote understanding and to render comparison with James and Gray (1986)  
9 more precisely, Figures S1, S2, and S3 display time-mean, zonal-mean variance of zonal,  
10 vertical, and meridional velocity decomposed into its contributions of the zonally averaged  
11 circulation and the eddy part of the flow. Whereas the latter is presumably dominated by  
12 synoptic-scale waves, the former contains annular mode-like variability and the meridional  
13 overturning circulation respectively. For vertical and meridional velocity the eddy flow  
14 variance experiences a strong decline over the whole range of friction time scales consistent  
15 with the suppression of baroclinic instability by the barotropic governor. In contrast, the  
16 decline of variance for zonal velocity is limited to friction time scales  $\tau_f > 2\text{days}$ . This  
17 is interesting regarding the effect of an eddy-mean flow feedback. Specifically, the power  
18 spectra in Figure 7 show a similar separation between the strong and weak friction cases  
19 where low-frequency variability is relatively stable for short and intermediate friction time  
20 scales ( $\tau_f \leq 2\text{days}$ ). For long friction time scales  $\tau_f > 2\text{days}$ , low-frequency variability  
21 declines more strongly indicating a disruption of the eddy-mean flow feedback.

# Appendix S2

22 In the context of the *signal-to-noise paradox* in seasonal prediction, the ratio of predictable  
23 components (*RCP*) as defined by Eade et al. (2014) is a useful measure with values larger

1 than one meaning that the model underestimates the magnitude of the predictable signal  
2 relative to internal noise. On seasonal time scales and for very large ensembles, the RCP  
3 approaches a value of three in current predictions systems (Baker et al., 2018), i.e. the  
4 signal-to-noise ratio is three times too small. The present study suggests that this deficit  
5 can be reduced by reducing mechanical damping (see Fig. 8, 9). The idealised experimental  
6 set-up we have used does not allow for a comparison with observations. However, we can  
7 compute the signal to noise ratio given by

$$\text{S2N} = \text{EM} / \sqrt{\sigma_{Nm}^2} \quad (\text{S1})$$

8 Here EM is the ensemble mean and  $\sigma_{Nm}$  is the ensemble spread about that mean. Also,  
9 since we are interested in the Rossby wave response to the tropical forcing, the zonal mean  
10 has been removed before computing S2N using equation (S1). The horizontal distribution of  
11 the ensemble spread is displayed in the lower panels of Figure S4 for each friction time scale  
12  $\tau_f$ . The distribution is largely zonally symmetric and it is the zonal mean of these fields  
13 that is shown in Figure 9. In the tropics, the spread is small compared to the extratropics  
14 which leads to large values of S2N, as can be seen from the upper panel for each friction  
15 time scale in Figure S4. Overall, we see an increase in S2N by a factor of three in the  
16 extratropics between the shortest and the longest friction time scale. This confirms that  
17 the barotropic governor has an influence on the signal-to-noise ratio and potentially on the  
18 signal-to-noise paradox discussed by Scaife and Smith (2018). Obviously, our experimental  
19 set-up is extremely simple and further work is required using more realistic models.

## 20 **References**

- 21 Baker, L., Shaffrey, L., Sutton, R., Weisheimer, A., and Scaife, A. (2018). An intercompari-  
22 son of skill and overconfidence/underconfidence of the wintertime north atlantic oscillation  
23 in multimodel seasonal forecasts. *Geophysical Research Letters*, 45(15):7808–7817.
- 24 Eade, R., Smith, D., Scaife, A., Wallace, E., Dunstone, N., Hermanson, L., and Robinson,

- 1 N. (2014). Do seasonal-to-decadal climate predictions underestimate the predictability of  
2 the real world? *Geophysical Research Letters*, 41(15):5620–5628.
- 3 James, I. and Gray, L. (1986). Concerning the effect of surface drag on the circulation of a  
4 baroclinic planetary atmosphere. *Quarterly Journal of the Royal Meteorological Society*,  
5 112(474):1231–1250.
- 6 Scaife, A. A. and Smith, D. (2018). A signal-to-noise paradox in climate science. *npj Climate  
7 and Atmospheric Science*, 1(1):1–8.

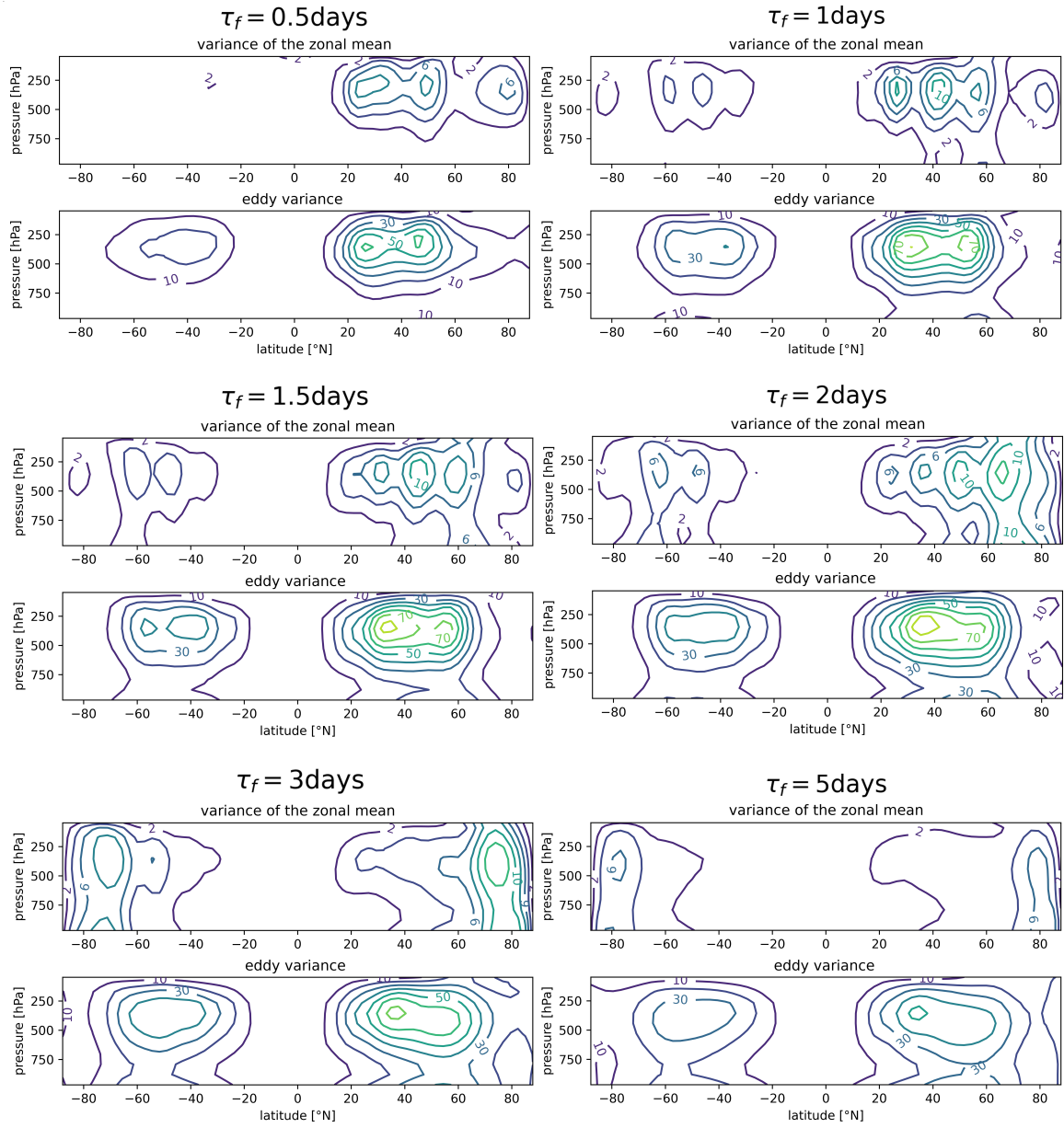


Figure S1: Time-mean variance of zonal wind for different aquaplanet configurations decomposed into contributions by the zonal-mean (contour spacing of  $10m^2s^{-2}$ ) and the eddy part of the flow (contour spacing of  $2m^2s^{-2}$ ).

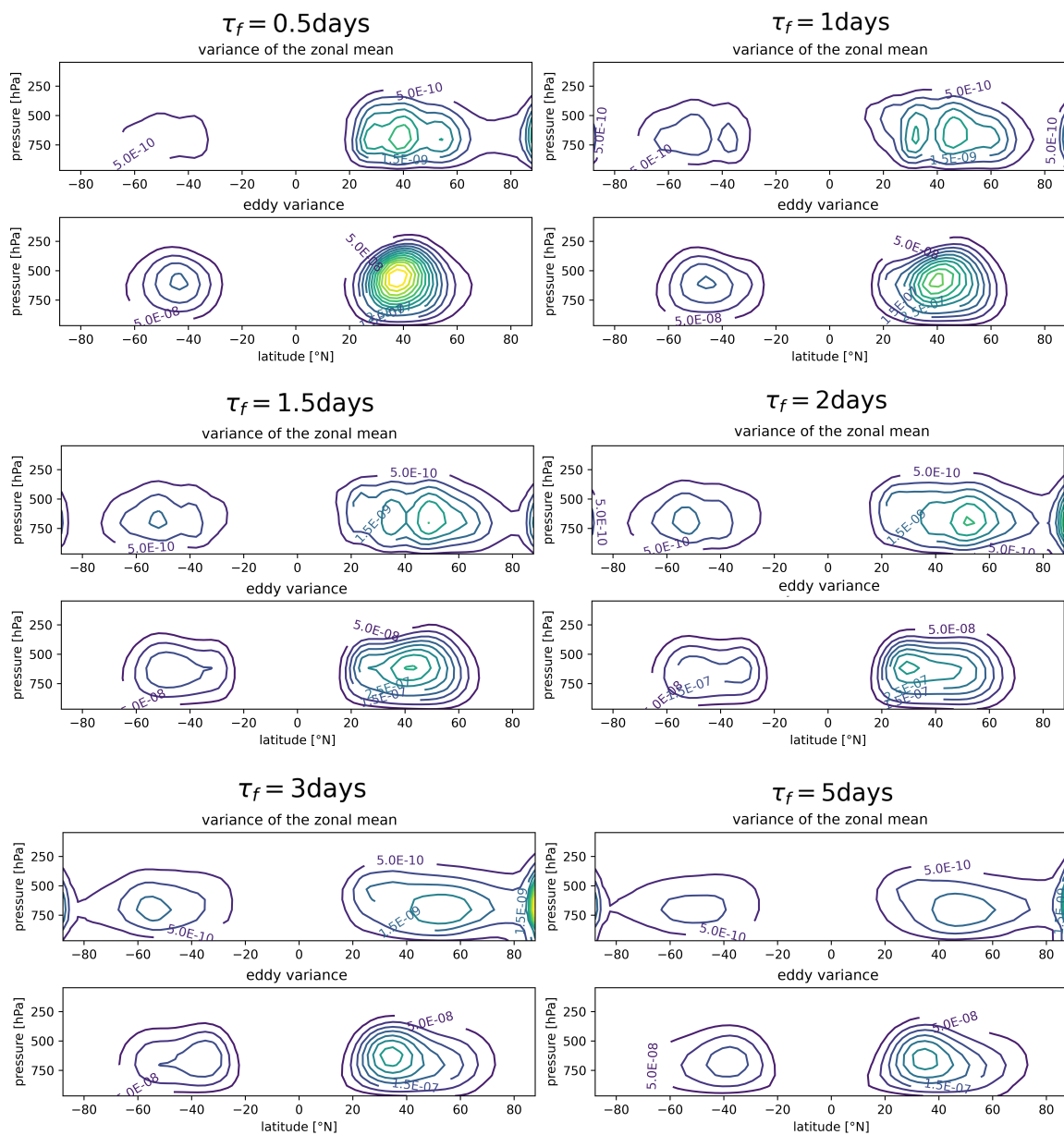


Figure S2: Like Figure S1 but for vertical wind with contour spacings of  $5E-08 \text{ Pa}^2 \text{ s}^{-2}$  and  $5E-10 \text{ Pa}^2 \text{ s}^{-2}$ , respectively.

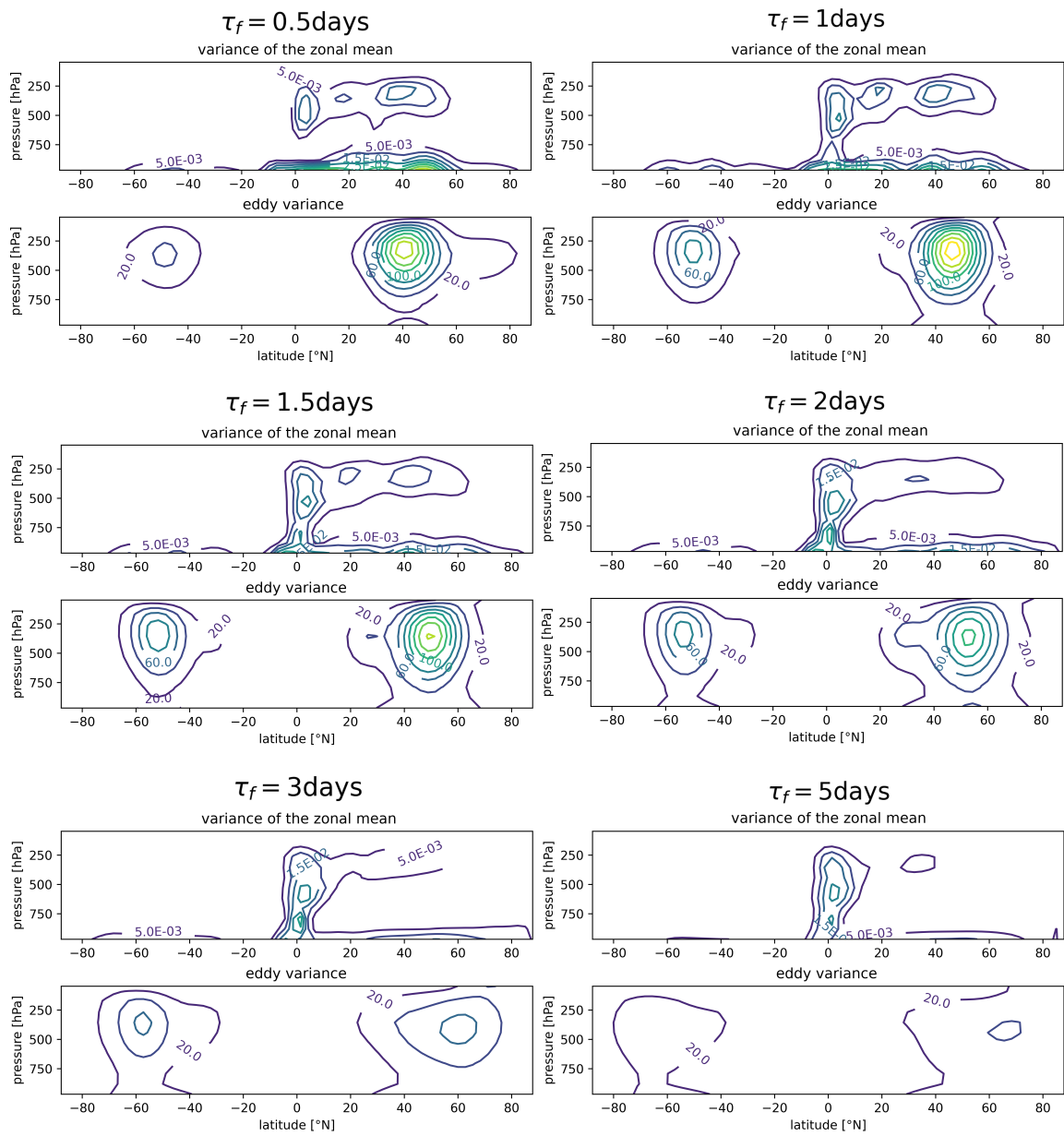


Figure S3: Like Figure S1 but for meridional wind with contour spacings of  $20 \text{ m}^2 \text{ s}^{-2}$  and  $0.005 \text{ m}^2 \text{ s}^{-2}$ , respectively.

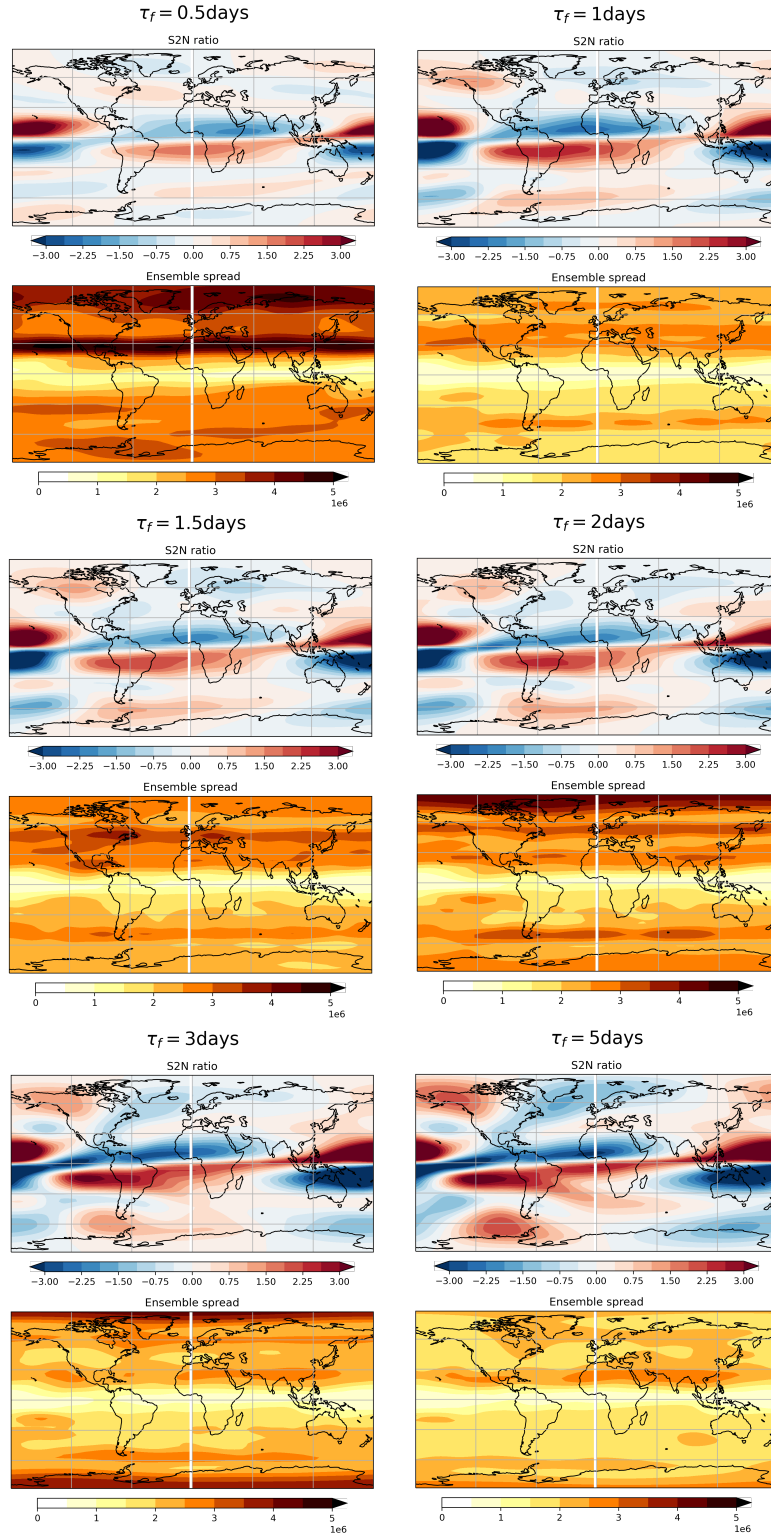


Figure S4: Signal-to-noise ratio as defined by equation S1 and ensemble spread measured by the standard deviation of 90-day mean streamfunction perturbations [ $m^2 s^{-1}$ ] at 357hPa for the simulations with tropical heating and different friction time scales  $\tau_f$ .